IVYSPRING INTERNATIONAL PUBLISHER

Theranostics

2017; 7(15): 3608-3623. doi: 10.7150/thno.21225

Review

Focused Ultrasound Immunotherapy for Central Nervous System Pathologies: Challenges and Opportunities

Colleen T. Curley[1*], Natasha D. Sheybani[1*], Timothy N. Bullock[2], and Richard J. Price[1]✉

1. Department of Biomedical Engineering, University of Virginia, Charlottesville, VA

2. Department of Pathology, University of Virginia, Charlottesville, VA

*Authors Contributed Equally

✉ Corresponding author: Richard J. Price, Department of Biomedical Engineering, Box 800759, Health System, Charlottesville, VA 22908; Phone: 434-924-0020; E-mail: rprice@virginia.edu

Received: 2017.05.28; Accepted: 2017.07.13; Published: 2017.08.23

Abstract

Immunotherapy is rapidly emerging as the cornerstone for the treatment of several forms of metastatic cancer, as well as for a host of other pathologies. Meanwhile, several new high-profile studies have uncovered remarkable linkages between the central nervous and immune systems. With these recent developments, harnessing the immune system for the treatment of brain pathologies is a promising strategy. Here, we contend that MR image-guided focused ultrasound (FUS) represents a noninvasive approach that will allow for favorable therapeutic immunomodulation in the setting of the central nervous system. One obstacle to effective immunotherapeutic drug delivery to the brain is the blood brain barrier (BBB), which refers to the specialized structure of brain capillaries that prevents transport of most therapeutics from the blood into brain tissue. When applied in the presence of circulating microbubbles, FUS can safely and transiently open the BBB to facilitate the delivery of immunotherapeutic agents into the brain parenchyma. Furthermore, it has been demonstrated that physical perturbations of the tissue microenvironment via FUS can modulate immune response in both normal and diseased tissue. In this review article, we provide an overview of FUS energy regimens and corresponding tissue bioeffects, followed by a review of the literature pertaining to FUS for therapeutic antibody delivery in normal brain and preclinical models of brain disease. We provide an overview of studies that demonstrate FUS-mediated immune modulation in both the brain and peripheral settings. Finally, we provide remarks on challenges facing FUS immunotherapy and opportunities for future expansion in this area.

Key words: focused ultrasound, immunotherapy, brain tumors, targeted drug and gene delivery

Introduction

The brain has long been considered a site of immune privilege. The limited ability of the immune system to respond to antigens within the brain parenchyma has been attributed to the absence of classical lymphatics, low major histocompatibility complex (MHC) expression, and small numbers of antigen presenting cells. However, recent findings, such as the discovery of functional meningeal lymphatic vessels, are redefining our perspective of how the immune and central nervous systems (CNS) interact[1,2]. Indeed, new evidence indicates that the immune and central nervous systems are more closely intertwined than previously thought, with the immune system playing a prominent role in shaping CNS development and function[3]. The immune system has also been implicated as a major influence

in numerous brain diseases. For example, in multiple sclerosis, autoreactive lymphocytes in the CNS facilitate oligodendrocyte demyelination, gliosis, and ultimately axonal degeneration[4]. In addition, chronic inflammation and innate immune system activation are common features of neurodegenerative diseases such as Alzheimer's and Parkinson's[5]. Gene expression studies in schizophrenia patients have shown alterations in both innate and adaptive immune signatures, and mood disorders such as depression have now been linked to inflammation[6,7]. Meanwhile, it has also been well-established that immunosuppression in the brain tumor microenvironment allows tumor cells to evade the immune system and escape clearance[8]. While consideration of the immune privilege status of the CNS has perhaps discouraged investigators from applying immunotherapies to the treatment of brain disorders in the past, we contend that these provocative new findings linking adaptive immunity to the CNS indicate that such approaches have considerable promise going forward.

While the immune component of many brain diseases is complex, stimulation of the immune system has shown some promise in treatment of cancer and neurodegenerative proteinopathies. In these settings, immune activation may lead to destruction and clearance of tumor cells or protein aggregates. Current strategies for enhancing immune system include vaccination, checkpoint inhibitors, and TLR agonists, such as CpG. Another promising approach for stimulating therapeutic immune responses in the brain is the deposition of high-density acoustic energy via non-invasive focused ultrasound (FUS)[9]. Typically performed under real-time image guidance using diagnostic ultrasound or MRI, FUS can markedly enhance therapeutic drug and gene delivery and distribution, as well as potentiate immune responses in tissues[10,11]. These outcomes of FUS can be attributed to a variety of bioeffects. In this review, we provide discussion of FUS energy deposition schemes and related bioeffects, an overview of the literature pertaining to FUS mediated delivery of antibodies to the brain, and evidence of FUS-induced immunomodulation in the brain and the periphery. We conclude by offering perspectives on new opportunities for the role of FUS in immune-based treatment of brain diseases.

Focused Ultrasound Energy Regimens for Immunotherapy

FUS serves as an attractive non-invasive tool for therapy and immune modulation due to the versatility of bioeffects that can be manifested at the focal spot. These mechanisms of action may be classified broadly as either "thermal" or "mechanical" in nature. Moreover, in most applications, FUS parameters may be precisely selected from within fairly wide ranges to generate varying intensities of thermal and mechanical energy deposition in tissue. In this section, we highlight thermal and mechanical FUS energy deposition regimens that are known to facilitate enhanced immunotherapeutic drug delivery and/or elicit anti-tumor immune responses.

Thermal FUS Regimens

When applied as a continuous wave, FUS can be used to deposit primarily thermal energy into tissue and tailored to either thermally ablate the tissue or create sub-ablative hyperthermia. The general characteristics of these thermal FUS regimens and their respective bioeffects are graphically summarized in Figure 1. Within the thermal ablation FUS regimen, FUS is applied to generate temperatures that are typically above 60°C, leading to nearly instantaneous onset of coagulative necrosis in the focal zone[12]. The signature of protein denaturation, membrane fusion, and nature of cell death in the context of FUS ablation is in part dictated by target tissue composition, as heat diffusion can play a role in mediating a temperature gradient in the periablative zone. In this transition zone between necrotic and viable tissue, cells do not receive a lethal thermal dose, but instead experience thermal stresses that ultimately give rise to alternative routes of cell death, such as apoptosis[13]. Clinical applications of FUS ablation cover a broad spectrum of disease types and locations, including neurodegenerative disorders and an assortment of solid tumors[10]. On the other hand, applying continuous wave FUS at much lower intensities can be used to yield sub-ablative hyperthermia. In this FUS regimen, the entire volume of a treated tissue or tumor may be heated, without immediately killing cells, by sweeping the ultrasound focus through the tumor volume. This lower intensity thermal FUS generates heat shock protein expression and triggers other mechanisms of anti-tumor immunity that will be described in further detail later in this review.

Mechanical FUS Regimens

Alternatively, FUS may be applied to generate predominantly mechanical bioeffects. The general characteristics of these mechanical FUS regimens and their respective bioeffects are graphically summarized in Figure 2. Generally speaking, mechanical bioeffects may be created by applying FUS using pulsed sequences, with FUS peak-negative pressure adjusted to manipulate bioeffect magnitude. When pulsed FUS is applied at high peak-negative pressures,

non-thermal destruction of tissues can occur through mechanical lysis of cells. The subcellular fragmentation of tissues often results in lesions with sharply delineated margins and little detectable cellular content[11]. These bioeffects are attributed to physical phenomena, such as acoustic cavitation, acoustic streaming/microstreaming, radiation force, and shear stresses that are induced in the ultrasound field[11]. Moreover, the mechanical consequences of acoustic cavitation are more pronounced in the presence of i.v. injected acoustic amplifiers, such as contrast agent microbubbles. When i.v. injected gas-filled microbubbles interact with an ultrasound field, they oscillate in either a stable or inertial manner. These two modes of oscillation, otherwise known as cavitation, refer to bubble activity in low- and high-pressure acoustic fields, respectively. Inertial cavitation occurs when these oscillations lose stability and ultimately lead to rapid, violent bubble collapse. In turn, this can yield a highly localized rise in temperature, acoustic streaming, and shock wave formation [14]. On the other hand, stable cavitation is a more predictable mode in which bubbles steadily oscillate in size to produce mechanical shear forces, as well as circumferential stresses, on microvessel walls. Of note, to date, stable cavitation has been the predominating mechanism for blood brain barrier (BBB) and/or blood-tumor barrier (BTB) opening in pre-clinical and clinical studies. Stable oscillation of systemically administered microbubbles has been shown to lead to transient tight junction opening, vascular endothelial sonoporation, and enhanced transcytotic capabilities spanning an estimated 4-6 hour period over which the BBB/BTB is open[14]. Of significance for immunotherapy, studies have capitalized on the potential use of FUS-mediated BBB opening as a tool for stimulating leukocyte extravasation into tissues[15–17]. These bioeffects of FUS have been harnessed to enhance delivery of antibodies, augment homing and accumulation of immune cells, and drive more robust basal immune responses to a host of pathologies, as will be discussed in greater depth throughout the remainder of this review.

Therapeutic Antibody Delivery Using FUS-Mediated Blood-Brain Barrier Opening

The blood brain barrier (BBB) prevents the transport of most systemically administered therapeutics to brain. Traditional options for increasing drug and/or gene delivery to CNS sites are either invasive, such as direct-injection or convection enhanced delivery (CED), or non-targeted, such as intra-arterial infusion of mannitol. FUS is a safe, non-invasive, and targeted method for BBB opening, and this approach has now been used by many labs to facilitate the delivery of agents such as chemotherapies, drug and gene-bearing polymeric nanoparticles, and antibodies to the brain[18–26]. Additionally, ultrasound has been shown to enhance pore size of extracellular and perivascular space, facilitating enhanced dispersion of therapeutics in brain tissue[27–32]. The degree of FUS-mediated BBB opening and efficacy of agent delivery depends on a number of factors, such as acoustic parameters, microbubble characteristics, and properties of the targeted brain region. For example, increased acoustic pressures facilitate delivery of larger agents into the tissue, and larger microbubble diameters result in enhanced delivery and successful BBB disruption at lower acoustic pressures[33,34]. Many other parameters have been explored in the literature; however, these studies are beyond the scope of this article. FUS+MB-mediated BBB opening has now moved into clinical trials, with initial results demonstrating safe BBB opening in glioblastoma patients when ultrasound is applied using an implanted device in the presence of intravenous microbubbles[35]. Another clinical trial, wherein microbubbles are activated for achieving drug delivery to gliomas in patients using a phased-array FUS system, is also well-underway (NCT02343991). Recently, antibodies targeted to immune regulatory molecules, known as checkpoint blockade antibodies, have had great success in the treatment of some peripheral cancers by reactivating immune responses to tumor antigens. Immune modulating antibodies targeted to the CNS may yield promising treatment strategies for brain diseases, and FUS is a powerful tool to augment delivery and therefore efficacy in the brain. Here, we illustrate this capability of FUS by reviewing the literature on focused ultrasound blood brain barrier opening for antibody delivery. Note that the studies discussed in the forthcoming sub-sections are summarized in Table 1.

BBB Opening of Normal Brain Tissue for Antibody Delivery

A number of studies have been performed in normal brain tissues confirming antibody delivery via BBB opening with FUS-activated microbubbles. Electron microscopy of brain regions exposed to FUS-mediated BBB opening has shown endothelial cells with increased number of vesicles and vacuoles, folds and invaginations on the luminal surface, cytoplasmic channels, and tight junction opening when compared to unsonicated regions. Immunoelectron microscopy has revealed the presence of endogenous IgG in the neuropil

surrounding vessels in sonicated samples, verifying passage of circulating antibodies across the blood brain barrier[36]. This technique has also been used to deliver systemically administered, functionally intact, D_4 receptor antibodies to localized regions of the normal mouse brain[19], as well as Herceptin (trastuzumab), a humanized anti-human epidermal growth factor receptor 2 (HER-2) monoclonal antibody used in the treatment of HER-2 positive breast cancer[20]. These studies demonstrate the utility of FUS as a tool for targeted and non-invasive delivery of antibodies across the blood brain barrier. As such, they open the door for more widespread use of FUS for delivery of therapeutic antibodies in preclinical models of brain disease.

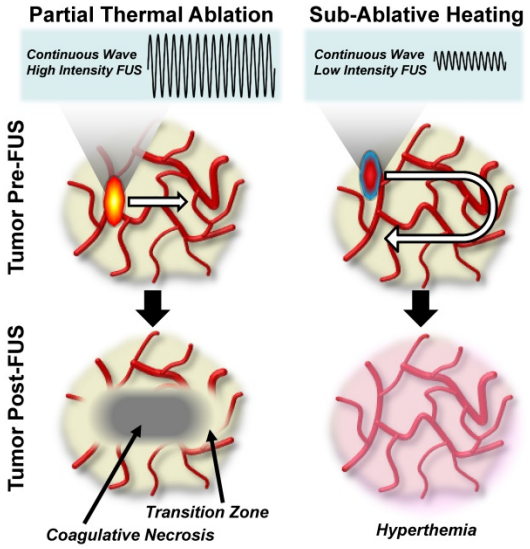

Figure 1. Thermal focused ultrasound energy regimens for cancer immunotherapy. *Left Column*: Partial thermal ablation using high-intensity continuous wave focused ultrasound. Sweeping the ultrasound focus through a pre-identified fraction of the tumor volume at these high energy levels generates a zone of coagulative necrosis, which is then surrounded by a zone of transition to normal tumor tissue. *Right Column*: Sub-ablative tissue heating using low-intensity continuous wave ultrasound. Sweeping the ultrasound focus through the entire tumor volume at this energy level elicits hyperthermia without immediately killing tumor cells.

BBB Opening for Treatment of Neurodegeneration with Antibodies

One such area of research has been the use of FUS-induced BBB opening for therapeutic antibody delivery in the pre-clinical treatment of neurodegenerative diseases. In two different transgenic models of Alzheimer's disease, FUS application yielded a roughly 3-fold increase in systemically administered anti-amyloid antibody localized to plaques[37]. A subsequent study showed therapeutic efficacy of this approach in the TgCRND8 mouse model of Alzheimer's disease, with FUS-mediated anti-amyloid beta delivery resulting in a 12% reduction in plaque number and 23% reduction of plaque size in the FUS treated hemisphere[38]. It was later shown, using this same animal model, that FUS-mediated BBB opening alone facilitates binding of endogenous antibodies to amyloid beta plaques, yielding reduced plaque load and activation of microglia[39]. Instead of targeting beta amyloid, a recent study designed an anti-tau single chain variable fragment (RN2N) to bind tau neurofibrillary tangles present in Alzheimer's disease. Administration of RN2N and microbubbles, with subsequent application of scanning ultrasound in a transgenic mouse model overexpressing tau protein, yielded an 11-fold increase in RN2N delivery, a reduction of anxiety-like behavior, and tau phosphorylation compared to groups wherein RN2N was administered without ultrasound. The RN2N alone group did reduce anxiety like behavior, and both the RN2N only and ultrasound only groups showed reduction in phosphorylated tau levels; however, all effects were greatest in the group receiving both ultrasound and RN2N[40]. Thus, focused ultrasound has been shown to be an effective approach for the delivery of antibody therapeutics in mouse models of Alzheimer's disease, and it is evident that FUS alone exerts beneficial effects that are capable of reducing plaque load.

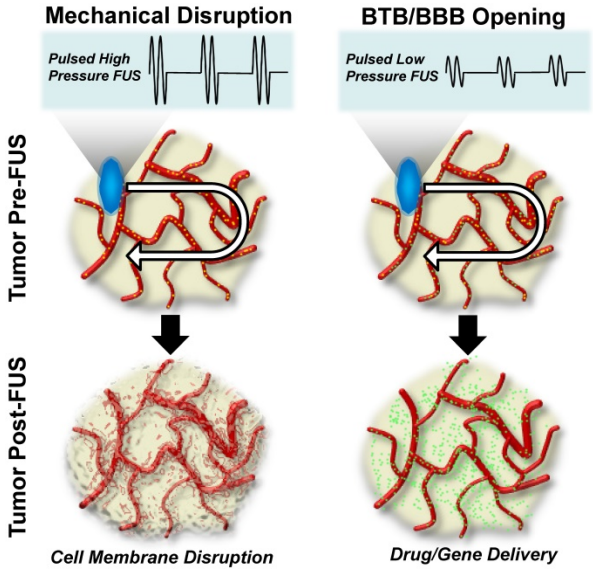

Figure 2. Mechanical focused ultrasound energy regimens for cancer immunotherapy. *Left Column*: Mechanical disruption using pulsed, high-pressure, focused ultrasound after intravenous injection of contrast agent microbubbles (top row: yellow dots evident in red blood vessels). Driving microbubbles into inertial cavitation by sweeping the ultrasound focus through the tumor volume disrupts cell membranes and mechanically injures tumor tissue. Due to the use of very low duty-cycles, this energy regimen is not typically associated with tumor heating. *Right Column*: Blood-brain and/or blood-tumor barrier opening for delivering systemically administered immunotherapeutic drugs (top row: green dots evident in red blood vessels) to the CNS using pulsed, low-pressure, focused ultrasound. Here, contrast agent microbubbles (top row: yellow dots evident in red blood vessels), which are i.v. injected with the immunotherapeutic drug, stably oscillate in the FUS field. Stable oscillations open the BBB/BTB, permitting targeted immunotherapeutic drug deliver to treated CNS tissue (bottom row; green dots).

FUS for Delivering Antibodies to Brain Tumors

Focused ultrasound has also been used for delivery of therapeutic anti-cancer antibodies in studies aimed at establishing experimental therapeutic efficacy for treating intracranial tumors. For example, the therapeutic efficacy of HER-2 targeting antibody delivery with FUS has been tested in a brain tumor metastasis model of HER-2 positive breast cancer. In this study, some animals received no treatment, while treatment groups included the HER-2 receptor targeting antibodies, trastuzimab and pertuzumab, i.v. administered with or without FUS-mediated BBB opening weekly for a 6-week period of time. A subset of animals in the FUS + antibody group were classified as responders, characterized by a slower tumor growth rate, while there were no responders in the antibody only group. There was increased survival in the FUS + antibody and antibody only groups compared to untreated animals, but no statistically significant difference between these two groups. No differences were seen between the responders and non-responders by the parameters measured in this study, but elucidating the determining factors between these two groups will likely be important if this approach will ever be translated to the clinic[41]. FUS has also been used for delivery of the anti-VEGFA monoclonal antibody, bevacizumab, in an intracranial glioma xenograft model. Weekly treatments with FUS, microbubbles, and bevacizumab resulted in decreased tumor growth, increased median overall survival, and decreased vessel area compared to untreated, FUS only, and bevacizumab only groups[42]. Beyond enhancing vascular permeability, there is evidence that ultrasound has effects in the extracellular space that can enhance therapeutic distribution in normal tissue[27–32].. Evidence in tumors is more limited, however, one study found increased distribution of directly administered gene carriers in a flank tumor model following ultrasound application. The authors noted increased pore size in the tumor extracellular space in ultrasound treated groups, and postulated that an increase in fluid conductivity in the extracellular space temporarily reduced interstitial fluid pressure within the tumor, contributing to enhanced plasmid distribution[43]. These findings demonstrate that FUS mediated BBB opening in intracranial tumors can increase efficacy of systemically administered therapeutic antibodies and may even broaden therapeutic antibody repertoire for brain malignancies by increasing penetration of previously ineffective therapies.

Table 1. Studies linking FUS-mediated blood-brain barrier opening to immunotherapy.

Reference	Model	Ultrasound Parameters	Key Observations
19	Mouse (swiss webster)	Frequency: 0.69 MHz Burst length: 10 ms Repetition frequency: 1 Hz Exposure length: 40 sec Acoustic Pressure:0.6 – 1.1 MPa Microbubble type: Optison	Delivery of D4 receptor antibody to mouse brain. No or minimal damage at 0.8 MPa or below. Major damage seen in some animals above 0.8 MPa.
20	Mouse (swiss webster)	Frequency: 0.69 MHz Burst length: 10 ms Repetition frequency: 1 Hz Exposure length: 40 s Acoustic Pressure: 0.6 and 0.8 MPa Microbubble type: Optison	Delivery of Herceptin. Significantly greater amount delivered at 0.8 MPa than 0.6 MPa
36	Rabbit (New Zealand white)	Frequency: 1.63 and 1.5 MHz Burst length: 100 ms Repetition frequency: 1 Hz Exposure length: 20 s Acoustic Power: 0.55 or 3 W Microbubble type: Optison	Sonication as 0.55 W resulted in increased vescicles and vacuoles in endothelial cells, fenestrae on EC luminal surface, and widened inter-endothelial cleft, and IgG was detected. Significant damage was seen at 3W.
37	Transgenic mice (B6C3-Tg and PDAPP)	Frequency: 0.69 MHz Burst length: 10 ms Repetition frequency: 1 Hz Exposure length: 40–45 s Acoustic Pressure: 0.67–0.8 MPa Estimated acoustic power: 0.28–0.4 W Microbubble type: Optison or Definity	Delivery of anti-Amyloid β antibodies in two different transgenic AD mouse models yielded a roughly 3-fold increase in antibody localized to plaques
38	TgCRND8 mice	Frequency: 0.558 MHz Burst length: 10 ms Repetition frequency: 1 Hz Exposure length: 120 s Acoustic Pressure: 0.3 MPa Microbubble type: Definity	Delivery of amyloid-β antibodies that colocalize with plaques on US treated hemisphere. In mice treated with FUS + anti-amyloid antibody, there was a 12% reduction in plaque number and 23% reduction of plaque size in the FUS treated hemisphere
39	non-Tg and TgCRND8 mice	Frequency: 0.5 MHz Burst length: 10 ms	FUS-mediated BBB opening alone facilitates binding of endogenous antibodies to amyloid beta plaques, yielding reduced plaque load and

Reference	Model	Ultrasound Parameters	Key Observations
		Repetition frequency: 1 Hz Exposure length: 120 s Acoustic Pressure: 0.3 MPa Microbubble type: Definity	activation of microglia
40	pR5 mice	Frequency: 1 MHz Burst length: 10 ms Repetition frequency: 10 Hz Exposure length: 6 s per spot Acoustic Pressure: 0.7 MPa Microbubble type: In-house, lipid-shelled	The entire forebrain of the mouse was sonicated by sequential 6 s sonications per spot. Administration of RN2N with microbubbles and scanning ultrasound yielded an 11-fold increase in RN2N delivery, a reduction of anxiety-like behavior, and tau phosphorylation compared to groups given RN2N was administered without ultrasound.
41	Nude rats (intracranial MDA-MB-361 cells)	Frequency: 690 kHz Burst length: 10 ms Repetition frequency: 1 Hz Exposure length: 60 s Acoustic Pressure: 0.46-0.62 MPa Acoustic Power: 0.4-0.7 W Microbubble type: Optison	A subset of animals in the FUS + antibody (trastuzimab and pertuzumab) showed slower tumor growth rate (responsders), while there were no responders in the antibody only group. There was increased survival in the FUS + antibody and antibody only groups compared to untreated animals, but no statistically significant difference between these two groups.
42	Nu/Nu mice (intracranial U87mg cells)	Frequency: 400 kHz Burst length: 10 ms Repetition frequency: 1 Hz Exposure length: 60 s Acoustic Pressure: 0.4-0.8 MPa Acoustic power = 4–18 W Microbubble type: Sonovue	Weekly treatments with FUS, microbubbles, and bevacizumab resulted in decreased tumor growth, increased median overall survival, and decreased vessel area compared to untreated, FUS only, and bevacizumab only groups
44	Sprague-Dawley rats (intracranial C6 glioma)	Frequency: 0.5 MHz Burst length: 100 ms Repetition frequency: 1 Hz Exposure length: 90 s Acoustic Pressure: 0.36-0.7 MPa Acoustic Power: 5 or 20 W Microbubble type: Sonovue	I.P. administration of IL-12 followed by application of FUS and microbubbles resulted in an approximately three-fold increase in IL-12 compared to untreated control mice. Mice receiving IL-12 with FUS had the highest CD8+/T-reg ratio, slowed tumor progression, and the greatest survival benefit
45	Athymic nude rat (intracranial MDA-MB-231 cells)	Frequency: 551.5 kHz Burst length: 10 ms Repetition frequency: 1 Hz Exposure length: 120 s Acoustic Pressure: 0.32-0.35 MPa Microbubble type: Definity	FUS administration generated a 10-fold increase in HER2-specific NK-92 cells abundance in the FUS-targeted region after i.v. NK-92 injection when compared to i.v. NK-92 injection without FUS
46	Athymic nude rat (intracranial MDA-MB-231 cells)	Frequency: 551.5 kHz Burst length: 10 ms Repetition frequency: 2 Hz Exposure length: 120 s Acoustic Power: Used a controller to monitor acoustic emissions and modulate acoustic power to predetermined ultraharmonic signatures. Microbubble type: Definity	With aggressive treatment schedule, animals in the FUS + NK-92 group showed a reduction in tumor growth and increase in survival compared to controls

FUS-Mediated Delivery of Immunomodulatory Agents and Cells

Immunomodulatory agents such as cytokines and targeted immune cells have also been delivered via FUS-mediated BBB opening for treatment of brain tumors. Intraperitoneal administration of IL-12 followed by application of FUS and microbubbles resulted in an approximately three-fold increase in IL-12 in an orthotopic glioma model compared to untreated control mice, whereas mice receiving IL-12 without FUS had roughly two-fold increase. Enhanced delivery of IL-12 with FUS generated the highest CD8+/T-reg ratio, slowed tumor progression, and the greatest survival benefit[44]. NK-92 cells are a human natural killer cell line that can be modified to target tumor associated antigens, such as HER-2. In an intracranial model of HER2 positive breast cancer metastasis, FUS administration generated a 10-fold increase in HER2-specific NK-92 cells abundance in the FUS-targeted region after i.v. NK-92 injection when compared to i.v. NK-92 injection without FUS[45]. With an aggressive treatment regimen consisting of five treatments in the first week, two in the second week, and one in the third week, animals in the FUS + NK-92 group showed a reduction in tumor growth and increase in survival compared to controls[46].Taken together, we contend that the studies reviewed here demonstrate that FUS is a versatile tool that facilitates delivery of antibody immunotherapies and other immunomodulatory agents to normal and diseased brain tissue.

Experimental & Clinical Evidence for Direct FUS-Mediated Immunomodulation

In addition to facilitating increased delivery and distribution of therapeutic agents in the brain, FUS has also been shown to have immune-related effects in both normal and diseased brain tissue, as well as in peripheral tumor tissue. In this section, we review

those few studies that have investigated these mechanisms in the brain and then turn to the larger body of literature in extracranial tumors for insight into how FUS-mediated immune mechanisms may be better exploited in the setting of the CNS.

FUS-Immunomodulation in the Brain

Most studies of FUS-mediated BBB opening have focused on using this approach to deliver therapeutic agents to the brain; however, it has also come to be appreciated that the procedure itself may exert some immune-related effects. In particular, two different studies have evaluated the molecular effects of focused ultrasound BBB opening in rat brains. The first profiled changes in RNA and protein expression at acute time points following FUS BBB opening. Here, increases in both HSP70 and proinflammatory cytokines were measured within 24 hours. An increase in Iba1 was also reported, indicating microglial activation, and macrophages from the periphery were found in the sonicated region at six days post-treatment[47]. Previously, macrophages had only been detected in the brain after sonicating at higher pressures that induced intracerebral hemorrhage; however, it should be noted that their analysis was limited to 24 hours following FUS[48]. The second study looked more specifically at RNA expression in brain endothelial cells following FUS-mediated BBB opening. At six hours post sonication, there was an upregulation of pro-inflammatory chemokine and cytokine genes and a downregulation of BBB related transporter genes, which mostly returned to baseline by 24 hours[49]. Both studies found increases in GFAP indicative of astrocyte activation. Astrocytes have been demonstrated to play a role in innate CNS immunity and implicated as MHC class II APCs capable of T cell activation[50,51]; thus, the tropism induced by BBB opening is a crucial component to understanding consequent immune responses in the brain.

Interestingly, FUS-mediated opening of the BBB with microbubbles, independent of the delivery of a drug and/or therapeutic gene, exerts beneficial effects in mouse models of Alzheimer's disease. Indeed, ultrasound treatment has shown reduced plaque load in two studies utilizing different transgenic mouse models[39,52]. In both studies, the treated region displayed increased markers of microglial activation and greater localization of amyloid beta within microglia, suggesting that ultrasound was able to facilitate phagocytic uptake of Aβ, thereby aiding plaque clearance. In the APP23 model, functional tests indicated memory restoration in treated mice[52]. A phase one clinical trial for evaluating safety and feasibility of FUS and microbubble BBB opening in Alzheimer's patients is currently in progress (NCT02986932). Within intracranial tumor models, FUS and microbubble application also has immunomodulatory effects. FUS treated glioma tumors exhibited an increase in the CD8+/T-reg ratio, a metric commonly correlated with improved patient outcome[44]. Based on this evidence, we argue that the immunomodulatory influence of BBB opening with FUS activated microbubbles may provide an opportunity for synergy of FUS and immune based therapeutics, which may generate a stronger clinical response. Naturally, the capacity for FUS to generate over-exuberant immune responses in the brain must also be carefully considered.

FUS-Immunomodulation Outside the CNS

In settings outside of the brain, several studies now indicate a substantial role for FUS in inducing anti-tumor immunity. Possible mechanisms of anti-tumor immunity include stimulation of tumor-specific inflammation, broadening of the spectrum of available tumor antigens, modulation of immunosuppressive cytokine expression, stimulation of leukocyte infiltration and activation, and/or the alleviation of immunological tolerance. Figure 3 outlines the so-called "cancer immunity cycle" and depicts several points at which we hypothesize FUS may intersect with this cycle. Below, we review the literature centered on the use of FUS for stimulating anti-tumor immunity in settings outside of the CNS. Note that the studies discussed in the forthcoming sub-sections are summarized in Table 2.

Pre-Clinical Studies Using FUS Thermal Ablation for Immunotherapy

The application of FUS in high-energy intensity thermal regimens has been shown to act along a number of biological pathways in order to yield appreciable immune responses. FUS upregulates the release of endogenous danger signals such as ATP and heat shock proteins[53–56], while human prostate cancer cells exposed to sublethal temperatures via transrectal FUS are capable of inducing increased Th1 cytokine release, decreased Th-2 cytokine release, and upregulation in stress protein expression localized to the periphery of thermal FUS lesions[57]. Studies using the B16F10 melanoma model show that the application of FUS to tumors can decrease circulating tumor cells and pulmonary metastasis nodules, while simultaneously upregulating circulating TNF-α and IFN-γ. FUS was additionally determined to downregulate miR-134 (a miRNA determined to inhibit CD86 expression on B16F10 cells), leading to activation of CD86 expression and conferral of a more potent anti-tumor response[58]. In a murine model of

H22 model of hepatocellular carcinoma, FUS ablation was demonstrated to confer tumor-specific immunity as indicated by a significant increase in tumor antigen-specific I CD8+ cells, quantified with MHC-class I tetramers, versus sham and control groups. The cytotoxic CD8+ T lymphocytes (CTL) were observed to significantly upregulate key cytokines such as TNF-α and IFN-γ. When CTL from FUS-treated animals were adoptively transferred into untreated tumor-bearing mice, significant reductions in tumor growth and greater cumulative survival were observed versus adoptive transfer of CTLs from sham or control mice[59]. In the same model and under similar exposure conditions, two additional studies were performed. In one study, it was determined that DCs can undergo activation and generate host specific antitumor immunity in response to complete FUS ablation. Immunization of mice with immature bone marrow-derived DCs primed with FUS-treated tumor debris or lysate led to a significant increase in mature DCs, IL-12 and IFN-γ secretion of CTLs. While H22 tumor challenge using this strategy conferred a significant reduction in tumor growth among FUS-ablated tumor groups versus controls, no analogous stratification in long term survival rates was observed[60]. In the second study, it was concluded that FUS-treated tumor debris can effectively serve as a vaccination strategy to confer specific protective immunity. The specificity of CTL response to this debris suggests that the viable tumor antigen remaining following FUS ablation can improve tumor immunogenicity. Moreover, the strongest responses in tumor rejection and cumulative survival were conferred by the group that received FUS ablation without additional intervention via vaccination, suggesting that preservation of endogenous danger signal release was more effective than FUS-treated tumor lysate or untreated tumor lysate vaccination strategies. Nonetheless, the latter two interventions did promote upregulation of MHC-II, CD80, and CD86 expression on immature bone marrow-derived DCs, as well as IL-12 and IFN-γ production *in vitro*[61].

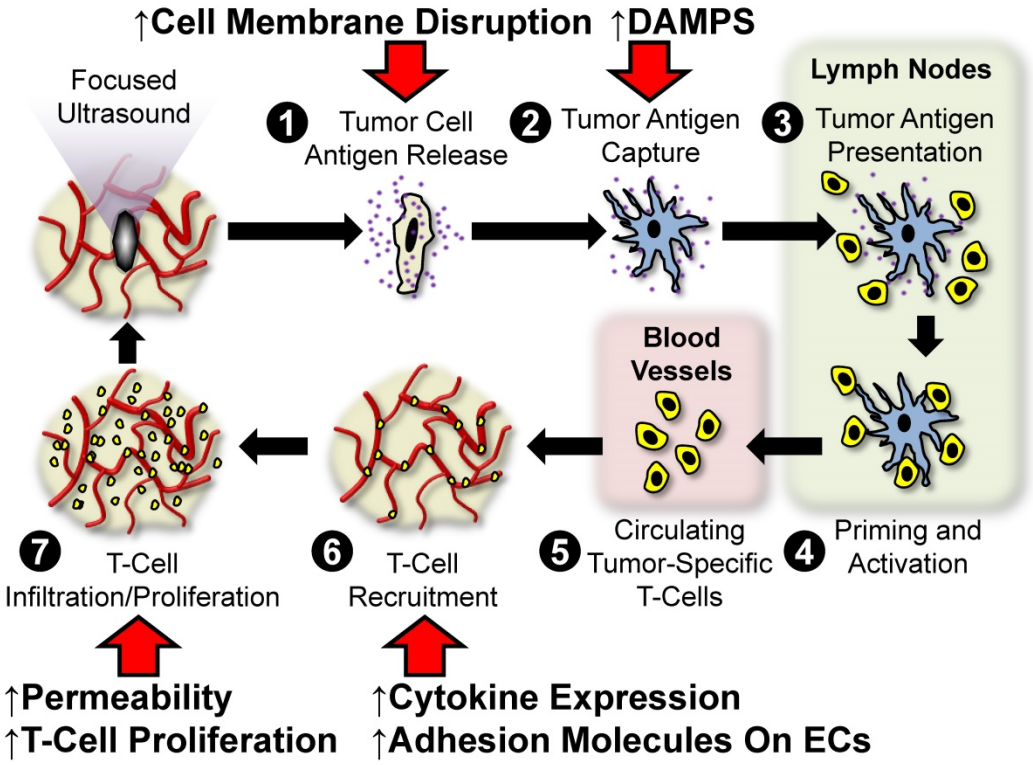

Figure 3. Hypothesized points of intersection between focused ultrasound and the cancer immunity cycle. In the cancer immunity cycle, antigens (purple) released from tumor cells (tan; 1) are captured by dendritic cells (blue; 2) and presented to T-cells (yellow 3) in lymph nodes (light green), leading to priming and activation of effector T-cells (4). Activated effector T-cells then pass into the systemic circulation (light pink; 5) and are trafficked to the tumor via adhesion to tumor endothelium (6). T-cells recruited from the circulation then infiltrate the tumor (7), where they specifically recognize and subsequently kill tumor cells. Tumor cell killing serves to release more antigen (1), allowing the cycle to continue. We hypothesize that focused ultrasound can trigger and/or boost anti-cancer immunity by intersecting at several points (red arrows) in this cycle. These include (i) enhanced tumor antigen release by cell membrane disruption, (ii) improved dendritic cell maturation via enhanced expression of damage associated molecular patterns (DAMPS), (iii) greater antigen flow to lymph nodes and less restricted intra-tumor T-cell migration as a result of mechanical disruption of stroma, and (iv) altered cytokine production, which may lead to augmented endothelial adhesion molecule expression and/or proliferation of intra-tumor T-cells.

Table 2. Studies of FUS-immunomodulation outside the CNS

	Ref	Year	Model	Ultrasound Parameters	Key Observations
Pre-Clinical and Clinical FUS Thermal Ablation.	53	2005	MC-38 mouse colon adenocarcinoma cell line	Frequency: 1.1 MHz Focal length: 63 mm Acoustic exposure conditions: **Thermal HIFU:** P- = 6.7 MPa, 30% duty cycle, 5 s **Mechanical HIFU:** P- = 10.7 MPa, 3% duty cycle, 30 s	HIFU treatment in vitro caused increased expression of ATP and Hsp60 APCs exposed to supernatant isolated from HIFU-treated tumor cells elevated CD80 and CD86 expression DCs and macrophages increased IL-12 and TNF-α secretion, respectively, in response to supernatant exposure Mechanical HIFU exposure condition surpassed its thermal counterpart in terms of ability to activate APCs
	54	2008	Reporter FVB mice transgenic for Hsp70-luc2A-eGFP	Frequency: 1.5 MHz Focal length: 5.1 cm Acoustic intensity: 53-352 W/cm² Exposure time: 1s	HIFU can induce Hsp70 expression up to 96 hours post-heating Peak expression levels are observed between 6-48 hours following exposure
	55	1998	LNCaP cells, prostatic stromal cells (in vitro studies) 5 patients with clinically localized prostate cancer (clinical studies)	**In vitro studies:** Sublethal heating at 43°C, 46°C, or 49°C for 60 min in a water bath **Clinical studies:** Frequency: 4.0 MHz Available focal lengths: 2.5, 3.0, 3.5, and 4.0 cm Acoustic intensity: 1,260–2,200 W/cm² Exposure time: 4s on followed by 12s off for re-positioning	Sublethal heat shock caused elevated Hsp27 expression by 3-4-fold in LNCaP cells Hsp27 expression was consistently observed at the borders of thermonecrosis in vivo, with strongest levels occurring at 2-3 hours following transrectal HIFU
	56	2006	23 patients with biopsy-proven breast cancer	Frequency: 1.6 MHz Focal length: 90 mm, Acoustic intensity: 5,000-15,000 W/cm² Exposure time: 45-150 mins (median: 1.3 h)	All tumors treated with HIFU stained positive for epithelial membrane antigen and Hsp70 No tumors treated with HIFU stained positive for CD44v6, MMP9, or PCNA
	57	2004	6 patients with clinically localized prostate cancer	Frequency: 4 MHz Focal lengths: 3.0, 3.5 or 4.0 cm Acoustic intensity: 1260-2000 W/cm² Exposure time: 4s on followed by 12s off for re-positioning	Hsp72, Hsp73, GRP-75, and GRP78 were overexpressed at the margins of HIFU treated regions
	58	2015	Subcutaneous B16F10 melanoma in female C57BL/6J mice	Frequency: 9.3 MHz Acoustic intensity: 4.5 W Focal length: Not provided Exposure time; 10s per location (120s total per tumor nodule)	HIFU treatment resulted in increased circulating TNF-α and IFN-γ, decreased circulating tumor cells, reduced pulmonary metastatic burden, and cumulative survival benefit. In vitro studies revealed a role for CD86 in driving anti-tumor immune effects in response to lifting of inhibition by miR-134.
	59	2012	Subcutaneous H22 hepatocellular carcinoma in female C57BL/6J mice	Frequency: 9.5 MHz Focal length: 8 mm Acoustic intensity: 5W Exposure time: 180-240s (median: 220s)	HIFU treatment elevated CTLs, TNF-α and IFN-γ secretion, and MHC class I/CD8+ cells versus sham and control
	60	2010	Subcutaneous H22 hepatocellular carcinoma in male and female C57BL/6J mice	Frequency: 9.5 MHz Focal length: 8 mm Acoustic intensity: 5 W Exposure time: 180-240s (median: 220s)	Mice immunized with DCs loaded with HIFU-ablated tumor lysate demonstrated increased magnitude of mature DCs and greater IL-12 and IFN-γ secretion compared to those immunized with mouse serum-loaded DCs. CTL cytotoxicity and TNF-α and IFN-γ secretion were significantly higher in mice immunized with HIFU tumor debris-loaded DCs.
	61	2010	Subcutaneous H22 hepatocellular carcinoma in male and female C57BL/6J mice	Frequency: 9.5 MHz Focal length: 8 mm Acoustic intensity: 5 W Exposure time: 180-240s (median: 220s)	Vaccination with HIFU-ablated tumor lysate resulted in elevated tumor-specific cytolytic activity compared to untreated tumor lysate vaccination, HIFU treatment alone, and control. HIFU-generated vaccine significantly reduced tumor growth and conferred 100% survival. Elevated expression of MHCII, CD80, CD86 and cytokine secretion (IL-12, IFN-γ) resulted from exposure of bone marrow DCs to HIFU-ablated or untreated tumor lysates in vitro.
	64	1992	Subcutaneous Cl300 neuroblastoma in male Ajax inbred mice	Frequency: 4 MHz Focal length: 8 cm Acoustic intensity: 550 W/cm² Exposure time: 5s on followed by 5s off	Tumors ablated with thermal HIFU underwent significant growth inhibition and extended survival compared to untreated controls. Mice challenged with contralateral tumors displayed secondary (untreated) tumor growth reduction in response to treatment of primary tumor with HIFU.
	65	2010	Subcutaneous MC38 colon adenocarcinoma and B16 melanoma in female C57BL/6 mice	Frequency: 3.3 MHz Focal length: 63 mm Acoustic intensity: P+ / P- = 19.5/7.2 MPa Exposure time: 4s	Application of thermal HIFU to tumors mediated greater recruitment of DCs to lesion periphery (<55 °C) than center (up to 80 °C), with spare-scan technique yielding stronger anti-tumor immune response compared to dense-scan technique
	66	2017	Orthotopic neu exon deletion line model of mammary adenocarcinoma in	Frequency: 3 MHz Focal length: Not provided Acoustic intensity: 5W (3.1 MPa) Scan speed: 1 revolution/s	Priming with immunotherapy 7 days prior to HIFU treatment resulted in decreased macrophages and MDSCs, increased CD8+ T cells secreting IFN-γ and PDL1+CD45+ cells, and elevated proportion of M1 macrophages

	Ref	Year	Model	Ultrasound Parameters	Key Observations
			FVB/n mice		Abscopal effect in the presence of increased tumor burden was more robust when immunotherapy priming preceded HIFU and lost when immunotherapy and HIFU were administered concomitantly.
	71	2009	48 female patients with biopsy-proven breast cancer	Frequency: 1.6 MHz Focal length: Not provided Acoustic intensity: 5,000- 15,000 W/cm² Exposure time: 45-150 mins (mean: 1.3 h)	Neoplasms treated with HIFU expressed elevated NK cells as well as CD3+, CD4+, CD8+, and B lymphocytes in the ablated periphery. TILs positive for granzyme, FasL, and perforin were also greater in response to HIFU as compared with untreated control tumors.
	72	2004	16 patients with solid malignancies (osteosarcoma, hepatocellular carcinoma, renal cell carcinoma)	Frequency: 0.8 MHz Focal length: 135 mm Acoustic intensity: 5000-20000 W/cm² Exposure time: Variable Therapeutic time: 2.5-8 h (median: 5.2 h)	Circulating CD4+ lymphocytes as well as the CD4+/CD8+ ratio increased in patients receiving HIFU
	73	2009	48 female patients with biopsy-proven breast cancer	Frequency: 1.6 MHz Focal length: Not provided Acoustic intensity: 5,000- 15,000 W/cm² Exposure time: 45-150 mins (mean: 1.3 h)	HIFU-treated tumors were observed to have APCs infiltrating along the margins of ablation, with an overall increase in DCs, macrophages, and B cells as compared with control. CD80, CD86, and HLA-DR were more highly expressed on DCs and macrophages infiltrating HIFU-treated tumors.
	74	2008	15 patients with solid malignancies	Frequency: 0.8 MHz Focal length: Not provided Acoustic intensity: 5000-20,000 W/cm² Exposure time: 0.78-3.62 h (mean: 2.74 h)	Patients exposed to complete or partial HIFU ablation experienced a reduction in serum immunosuppressive cytokine expression levels, with nonmetastatic patients experiencing lower expression levels as compared with metastatic patients VEGF, TGF-β1, and TGF-β2 were significantly reduced following HIFU treatment
Pre-Clinical FUS Mechanical Ablation.	63	2012	Subcutaneous RM-9 prostate cancer in C57BL/6J mice	Frequency: 3.3 MHz Focal length: Not provided Acoustic intensity: P+ / P- = 32/10 MPa (60 W) Exposure time: 20s (2% duty cycle)	Mechanical HIFU treatment (<45°C) and subsequent primary tumor resection attenuated intratumoral STAT3 activity, resulting in increased CTLs in spleens and TDLNs, and tumor growth inhibition upon rechallenge Number and activity of DCs was increased as a function of HIFU+surgery compared to surgery alone while immunosuppressive burden was alleviated
	67	2007	Subcutaneous H22 hepatocellular carcinoma in male and female C57BL/6J mice	Frequency: 3.3 MHz Focal length: 63 mm Acoustic exposure conditions: **Thermal HIFU** P+ / P- = 19.9/7.7 MPa, 3s **Mechanical HIFU** P+ / P- = 34.1/12.5 MPa, 2% duty cycle, 30s	Ablation with thermal and mechanical HIFU resulted in 3.1- and 4.1-fold increases in CD11c+ DCs, respectively, and 5- and 10-fold increases in TDLN CFSE+ DC accumulation, respectively. Both ablative protocols controlled tumor growth and conferred protection against tumor rechallenge Tumors ablated under mechanical HIFU protocol had stronger elevation tumor-specific CTL activity and IFN-γ secreting cells
	17	2012	Subcutaneous CT-26 colon carcinoma in BALB/cByJNarl mice	Frequency: 0.5 MHz Focal length: Not provided Acoustic intensity: P- = 0.6 MPa (5 We) or 1.4 MPa (30 We) Exposure time:20s (total sonication time between 180-240s) Microbubble type: Sonovue	Tumors exposed to low-intensity FUS and microbubbles experienced a transient increase in non-regulatory T cell infiltration as well as sustained elevation of CTLs, which further translated to restriction of tumor growth.
	68	2015	Subcutaneous K1735 melanoma in C3H/HeN mice	Frequency: 3 MHz (unfocused) Acoustic intensity: 2.3 W/cm² (0.22 MPa) Exposure time: 1 or 3 mins Microbubble type: Definity	Low-intensity antivascular US treatment significantly reduced tumor perfusion at both exposure times, while increasing HIF1A+ cells and CD45+CD3+ T cell infiltration in tumors
Pre-Clinical Low-Intensity FUS.	69	2016	B16 melanoma in C57BL/6 and BALB/c nude mice	Frequency: 1 MHz **Non-ablative low-intensity FUS:** Focal length: 80* or 85** mm Exposure time: 1.5 s (5 min total per tumor) Acoustic intensity: 550 W/cm2 *P- = 2.93 MPa (3W) **P- = 3.81 MPa (3W) **High-intensity ablation** Focal length: 80 mm Exposure time: 4s (75% duty cycle) Acoustic intensity: P- = 5.42 MPa (12.5W)	Non-ablative, low-intensity FUS conferred increased tumor antigen presentation and Hsp70 presence on tumor cell membranes, and led to reversal of T cell tolerance within tumors. Combination of this regimen with fractionated radiation therapy led to control of pulmonary metastatic burden and extended recurrence-free survival.
	70	2015	Orthotopic neu exon deletion line model of mammary adenocarcinoma in FVB/n mice	Frequency: 1.54 MHz Focal length: Not provided Acoustic intensity: P- = 1.1 MPa Exposure time: 5 mins	In mice with multiple tumor sites, the combination of ultrasound with copper-doxorubicin liposomes and CpG controlled tumor growth and extended survival in the context of systemic disease. CD4+ and CD8+ T cell magnitudes increased and MDSCs

Ref	Year	Model	Ultrasound Parameters	Key Observations
				decreased as a function of treatment in both primary (treated) and contralateral tumors.
16	2015	Subcutaneous xenograft model of CEA-expressing LS-174T human colorectal adenocarcinoma in female NSG mice	Frequency: 510 kHz Focal length: Not provided Acoustic intensity: 0.25 and 0.5 MPa Exposure time: 10 ms every second for 1 min; Microbubble type: Optison	Low-intensity focused ultrasound with microbubbles conferred significant accumulation of adoptively transferred iron-oxide labeled human NK cells at 0.5 MPa. Accumulation in the tumors lasted up to 24 hours.

Immunotherapeutic mechanisms were also speculated in a study demonstrating that debulking of unresectable neuroblastoma using FUS thermal ablation conferred a significant reduction in tumor growth when mice were challenged with a second tumor that did not receive further treatment following curative FUS treatment of the primary tumor. Though no additional analysis was conducted to confirm the role of a postulated antitumor immune response at that time, this study suggests that the application of FUS to stimulate immune response in the brain merits further exploration [62]. Beyond the brain, many pre-clinical and clinical studies have shed light on potential mechanisms of antitumor immunity conferred through the application of FUS to peripheral tumors.

Pre-Clinical Studies Using FUS Mechanical Disruption for Immunotherapy

Fewer studies examining the role of mechanical disruption with FUS on anti-cancer immunity have been performed; however, there is clear evidence that this FUS energy regimen may be efficacious for immunotherapy. In a model of RM-9 prostate cancer, mechanical FUS downregulated constitutively activated STAT3, the activation of which is implicated in immunosuppression[63]. Additionally, mechanical FUS with and without subsequent surgical resection appeared to eliminate tumor recurrence and/or distant metastasis, though mechanical FUS with surgery conferred the additional benefit of decreasing immunosuppression and upregulating DC magnitude and function. Application of mechanical FUS mediated an increase in tumor-specific CTLs in the spleen and tumor draining lymph nodes, which translated to greater survival benefit in recipient hosts[64]. Collectively, these findings allude to a potential interplay between the nature of direct tumor obliteration using FUS and subsequent release of danger signals and alleviation of immunosuppressive mechanisms that can lead to more robust anti-tumor immunity.

Pre-Clinical Comparisons of FUS Energy Regimens for Immunotherapy

Given the wide parameter space that exists for FUS applications, it is of note that some exposure conditions might be better suited for modulating immune response than others. Within the confines of thermal ablation alone, researchers have begun to address this matter. In MC-38 and B16 melanoma tumors, the implication of FUS scan pattern on quality of antitumor immunity has been tested. Sparse scan patterns yielded greater DC infiltration into lesion periphery (where the tumor cells were heated to ~55°C versus 80°C in tumor bulk) and significantly increased *in situ* maturation as compared with a dense scan pattern, perhaps by preserving antigen and alarmin integrity compared to coagulative approaches [65]. Consistent with findings in other peripheral tumor models, FUS thermal ablation also led to significantly increased IFN-γ+CD4+ T cells and CD8+ T cells and significantly decreased Tregs in a murine NDL model of epithelial mammary adenocarcinoma. However, when FUS was interlaced with adjuvant immunotherapy in this model, no abscopal effect was generated potentially due to the unexpected recruitment of immature myeloid cells by the thermal ablation protocol. The abscopal immune response to single or multisite thermal ablation was restored in distant, untreated tumors when the immune system was first primed with immunotherapy alone followed by a coincident thermal ablation and immunotherapy regimen[66]. Taken together, these results suggest that FUS exposure conditions, pattern of delivery, and timing of delivery can strongly dictate the immunogenicity of the treatment regimen, but also highlights the likelihood that sonication of immunosuppressed tumors may have little benefit without attending to the nature of the immunosuppression and anti-inflammatory responses that may arise as a function of the treatment regimen.

In the interest of characterizing how different FUS bioeffects may yield tunable immune readouts, a handful of studies have compared divergences in antitumor immune response between thermal and mechanical FUS. It has been demonstrated *in vitro* that FUS stimulates endogenous signal release (e.g. ATP, HSP60) from MC-38 murine prostate tumor cells. Exposure of APCs to supernatant of treated tumors cells additionally led to upregulation in costimulatory molecule expression, and increased IL-12 and TNF-α secretion by DCs and macrophages, respectively. When FUS-mediated mechanical lysis and thermal necrosis were directly compared in the context of

these readouts, the mechanical FUS regimen outperformed its thermal counterpart in yielding more plentiful endogenous danger signals and resultantly robust APC activation [53]. These results were recapitulated in MC38 tumors *in vivo*. Both thermal and mechanical FUS exposure conditions were capable of eliciting a systemic anti-tumor immune response illustrated by an increase in DC frequency and activation in the tumor draining lymph nodes. This phenomenon translated to significant reductions in growth of FUS-treated tumors versus controls, increased CTL activity, and protection against subsequent subcutaneous tumor re-challenge. Overall, mechanically predominated FUS lesions appeared to render more marked DC activation as compared with their thermally predominated counterparts[67].

Importantly, these findings highlight the potential negative impacts of ablative FUS regimens on anti-tumor immune response. Since the adaptive immune response against tumors is triggered more robustly by an immunogenic cell death, downstream effects of thermal FUS - such as coagulative necrosis and heat fixation - may hold undesirable implications for anti-tumor immunity. Following application of high-intensity thermal FUS, heat fixation typically occurs in the center of the lesion. The lethal temperatures reached at the focal region may also denature and thus diminish the availability of viable tumor antigen. In the periphery of the treated region, however, more abundant viable antigen and cells in an apoptotic state are commonly observed [13]. Taken together, these studies suggest that the selection of FUS regimen and associated parameters are of paramount importance for immunotherapy.

Low-Intensity FUS for Immunotherapy in Pre-Clinical Studies

A few select studies have also elucidated a role for non-ablative FUS in evoking anti-tumor immunity. In a murine CT-26 colon carcinoma model, low-pressure, pulsed ultrasound concomitant with microbubbles - an established regimen for permeabilization of tumor vasculature – upregulated sustained CD8+ CTL and transient effector CD4+ infiltration. Since Treg frequency was unchanged as a function of the ultrasound regimens applied, overall CD8+/Treg proportions increased significantly, conferring a transient inhibition in tumor growth within the first few days of treatment[17]. Similarly, in a K1735 model of melanoma, the application of antivascular low-intensity unfocused ultrasound with microbubbles conferred a statistically significant increase in CD45+ and CD3+ cells over sham tumors treated with ultrasound alone [68]. Notable trends in increased lymphocyte frequency were observed in a B16 melanoma model in which FUS was used as a method for generating an autologous tumor vaccine, eliciting tumor antigen presentation and reversing T cell tolerance. When combined with hypofractionated radiotherapy, FUS was demonstrated to confer primary tumor growth control, significant reduction in pulmonary metastases, and improved recurrence free survival[69]. Priming with non-ablative FUS was postulated to render a more strongly immunogenic tumor cell death following radiotherapy and yield a protective effect against local and distal metastasis. Though the putative mechanisms linking low intensity FUS to immunotherapy continue to be poorly understood, it was postulated that this effect was owing to stimulation of DC-driven priming of tumor antigen-specific T cells otherwise susceptible to tolerance [69]. In an NDL model of epithelial mammary adenocarcinoma, the delivery of CpG and temperature sensitive copper-doxorubicin (CuDox) liposomes conferred markedly elevated CD8+ and CD4+ T cell infiltration and reduction in myeloid derived suppressor cell (MDSC) burden in primary and contralateral tumor sites when combined with sub-ablative FUS [70]. Aside from stimulating the basal immune cell population in tumors, there also exists potential for supplementing the immune system by harnessing FUS for exogenous immune cell delivery as a means of multimodal immunotherapy. In a murine xenograft model of human colorectal adenocarcinoma, low-dose FUS with microbubbles was shown to potentiate homing and accumulation of systemically administered superparamagnetic iron oxide particle-labeled human NK cells in the tumor microenvironment[16].

Clinical Studies Examining the Impact of FUS on Aspects of Immunity

In the clinical setting, a number of studies have already demonstrated a role for FUS in stimulating antitumor immunity. For instance, breast neoplasms treated with FUS exhibited a marked increase in infiltration of activated TILs (specifically CD3, CD4, CD8, CD4/CD8 ratio, and B) and NK cells around the ablated lesion when compared with untreated neoplasms on examination following radical mastectomy. In the same samples, TILs were also functionally enhanced in the FUS group, displaying significant increases in FasL, granzyme, and perforin expression versus control[71]. Similar trends have been noted in patients with other solid tumor types. Circulating lymphocyte levels (specifically, CD4+ T cells and CD4+/CD8+ lymphocyte ratio) were elevated as a function of FUS ablation[72]. A more recent study involving immunohistochemical analysis

of biopsied human breast cancer tissues has delineated clear residual zones of viable tumor antigen embedded within FUS-ablated debris. It was posited that these antigens - most strikingly, epithelial membrane antigen - and well as upregulated HSP-70 can serve as mediators of enhanced antitumor immunity[56]. In a similar vein, FUS ablation has been demonstrated to increase tumor-infiltrating APCs in human breast cancer patients. FUS ablation of the primary breast cancer elicited significantly enhanced DC, macrophage, and B lymphocyte frequencies in the peri-ablative zone, with a large fraction of DC and macrophages expressing markers for activation[73]. Meanwhile, in patients with solid malignancies, FUS has been shown to decrease immunosuppressive serum cytokine levels, including significant decreases in TGF-β1, TGF-β2, and VEGF. In metastatic patients, only the trend in TGF-β2 decrease was sustained at a level of significance, while in non-metastatic patients, the aforementioned serum cytokine levels were decreased along with IL-6. Such findings suggest a correlation between tumor burden following FUS-mediated ablation and serum cytokine levels[74]. These early clinical results suggest that thermal FUS may have multiple roles in the cancer immunity cycle, with demonstrated potential to impact antigen presentation and danger signal release, APC activation, as well as lymphocyte infiltration into the tumor microenvironment.

Challenges Going Forward

Intersections between the immune and central nervous systems are becoming elucidated rapidly; however, they are still complex and still incompletely understood. The varied roles of the immune system in a myriad of CNS diseases will need to be better understood to most effectively implement immune based therapies. In Alzheimer's disease, for example, studies have postulated both beneficial and detrimental roles of the immune system in disease progression, and pre-clinical treatment strategies have included both immunosuppressive and immune activating agents[75]. For cancer applications, enhancing the anti-tumor immune response is an effective treatment approach as proven by the success of checkpoint blockade antibodies. These antibodies only work well in a subset of patients likely due to either the lack of immune recognition or other mechanisms of immune evasion. For successful use of immune-modulating antibodies within brain malignancies, it will be important to understand the array of immune evasion mechanisms. Beyond suppression within the tumor microenvironment, it has also been shown that intracranial tumors can hinder effector function of T-cells by way of systemic tolerance[76]. Additionally, though important to the discussion of FUS applications in cancer immunomodulation, the nuances of how the immune system responds to antigens in the brain are still not fully understood; this provides an additional challenge for tuning therapeutically relevant immune responses in the brain, and highlights the need to compare "successful" and unsuccessful FUS regimens to identify true biomarkers of therapeutic efficacy. Furthermore, although many of the studies listed above describe the ability to FUS regimens to promote the effector arm of the immune systems, very little characterization of mechanisms of adaptive resistance, such as the recruitment of immunosuppressive cells that are induced by acoustic energy, has been performed in brain or other tumor types. As discussed previously, clinical trials of FUS + MB BBB opening are currently in progress and thus far have demonstrated safety of this procedure at the tested parameters. It is possible, though, that more aggressive FUS parameters will be necessary to obtain the desired immune modulation for certain applications. In this case, safety will need to be carefully considered. In pre-clinical animal models, aggressive FUS parameters have resulted in vascular damage due to microbubble inertial cavitation. Damage can range from minor, consisting of small areas of red blood cell extravasation, to major vascular damage resulting in hemorrhage. Such vascular damage could, in turn, possibly lead to increased intracranial pressure and swelling. Additionally, with any method of immune stimulation, there are risks associated with over-activation of the immune system, such as autoimmunity.

Opportunities for the Future

The demonstration of efficacy in delivery of antibodies to the CNS using FUS has paved the way for interfacing this modality with other immunologically relevant adjuvants. Of note, within this class of therapeutics are checkpoint inhibitors. Checkpoint blockade antibodies, such as PD-1 and CTLA-4, have demonstrated high efficacy for some extracranial tumors[77]. Preclinical and anecdotal clinical evidence exist showing benefit from treatment of brain malignancies with checkpoint blockade antibodies[78–82]. As reviewed above, FUS has been used for delivery of antibodies to the brain, and thus has the potential to enhance efficacy of immune-modulating antibodies by increasing their concentrations at the desired site. Beyond antibodies, larger vehicles for drug and gene delivery, such as liposomes, polymeric nanoparticles, and virus can also be delivered across the BBB with FUS[23–26,83–86]. The capability of targeted delivery

of gene vectors opens up possibilities for altering immune stimuli within the diseased tissue. For example, immune signaling hubs within cells could be targeted by enhancing or knocking down expression of proteins using delivery of genes for transcription factors, microRNAs or anti-microRNAs, shRNAs.

The physical mechanisms of FUS application alone can perturb tissue in unique ways, bearing an impact on the immune milieu in and around targeted disease sites. To date, studies have yet to demonstrate a clear role for FUS as a monotherapy for achieving immunological tumor control. However, with appropriate FUS exposure conditions, it may be possible to enhance the effects of immunotherapies not only via improved delivery, but also through any synergies between FUS and therapeutic immune modulation. Radiotherapy (RT) has immunomodulatory properties and has shown promise in combination with a variety of immunotherapeutic approaches for treatment of non-brain malignancies[87–92]. In pre-clinical glioma models, RT has shown efficacy in combination with monoclonal antibody therapy, including checkpoint inhibition [93–96]. The combined effect is thought to come from radiation-induced cell damage capable of yielding immunologically favorable outcomes, such as immunogenic cell death, increased expression of MHC molecules and CD80, and release of immune stimulating cytokines and danger signals, which can activate dendritic cells and stimulate an immune response. RT can also induce the release of tumor associated antigens and change aspects of the tumor microenvironment to facilitate trafficking of immune cells into the tumor[93,97–99]. As discussed in this review, FUS is fully capable of conferring similar effects, such as stimulating the release of cytokines, danger signals, tumor associated antigens, and altering transport within tumors, without the harmful use of ionizing radiation, yet with added advantage of enhanced therapy/payload delivery to the tumor microenvironment. Therefore, going forward, we anticipate that FUS will emerge as an attractive modality to use in combination with immune based therapies for treating pathologies of the CNS.

Acknowledgements

Supported by NIH R01CA197111 and NIH R01EB020147.

Competing Interests

The authors have declared that no competing interest exists.

References

1. Louveau A, Harris T, Kipnis J. Revisiting the concept of CNS immune privilege. Trends Immunol. 2016;8:583–92.
2. Louveau A, Smirnov I, Keyes TJ, et al. Structural and functional features of central nervous system lymphatics. Nature. 2016;523:337–41.
3. Filiano AJ, Gadani SP, Kipnis J. Interactions of innate and adaptive immunity in brain development and function. Brain Res. 2015;1617:18–27.
4. Dendrou CA, Fugger L, Friese MA. Immunopathology of multiple sclerosis. Nat Rev Immunol. 2015;15:545–58.
5. Heneka MT, Kummer MP, Latz E. Innate immune activation in neurodegenerative disease. Nat Rev Immunol. 2014;14:463–77.
6. Badalà F, Nouri-mahdavi K, Raoof DA. Immune system disturbances in schizophrenia. Biol Psychiatry. 2008;144:724–32.
7. Hodes GE, Kana V, Menard C, et al. Neuroimmune mechanisms of depression. Nat Neurosci. 2015;18:1386–93.
8. Nduom EK, Weller M, Heimberger AB. Immunosuppressive mechanisms in glioblastoma. Neuro Oncol. 2015;17 Suppl 7:vii9-vii14.
9. Jagannathan J, Sanghvi NK, Crum LA, et al. High intensity focused ultrasound surgery (HIFU) of the brain: A historical perspective, with modern applications. Neurosurgery. 2009;64:201–11.
10. Kennedy JE. High-intensity focused ultrasound in the treatment of solid tumours. Nat Rev Cancer. 2005;5:321–7.
11. Jang HJ, Lee J-Y, Lee D-H, et al. Current and future clinical applications of high-intensity focused ultrasound (HIFU) for pancreatic cancer. Gut Liver. 2010;4:S57-61.
12. Zhou Y-F. High intensity focused ultrasound in clinical tumor ablation. World J Clin Oncol. 2011;2:8–27.
13. Hoogenboom M, Eikelenboom D, den Brok MH, et al. In vivo MR guided boiling histotripsy in a mouse tumor model evaluated by MRI and histopathology. NMR Biomed. 2016;29:721–31.
14. Timbie KF, Mead BP, Price RJ. Drug and gene delivery across the blood-brain barrier with focused ultrasound. J Control Release. 2015;219:61–75.
15. Vestweber D. Relevance of endothelial junctions in leukocyte extravasation and vascular permeability. Ann N Y Acad Sci. 2012;1257:184–92.
16. Sta Maria NS, Barnes SR, Weist MR, et al. Low dose focused ultrasound induces enhanced tumor accumulation of natural killer cells. PLoS One. 2015;10:1–17.
17. Liu H-L, Hsieh H-Y, Lu L-A, et al. Low-pressure pulsed focused ultrasound with microbubbles promotes an anticancer immunological response. J Transl Med. 2012;10:221.
18. Treat LH, McDannold N, Vykhodtseva N, et al. Targeted delivery of doxorubicin to the rat brain at therapeutic levels using MRI-guided focused ultrasound. Int J Cancer. 2007;121:901–7.
19. Kinoshita M, McDannold N, Jolesz FA, et al. Targeted delivery of antibodies through the blood–brain barrier by MRI-guided focused ultrasound. Biochem Biophys Res Commun. 2006;340:1085–90.
20. Kinoshita M, McDannold N, Jolesz FA, et al. Noninvasive localized delivery of Herceptin to the mouse brain by MRI-guided focused ultrasound-induced blood-brain barrier disruption. Proc Natl Acad Sci U S A. 2006;103:11719–23.
21. Etame AB, Diaz RJ, O'Reilly MA, et al. Enhanced delivery of gold nanoparticles with therapeutic potential into the brain using MRI-guided focused ultrasound. Nanomedicine. 2012;8:1133–42.
22. Samiotaki G, Acosta C, Wang S, et al. Enhanced delivery and bioactivity of the neurturin neurotrophic factor through focused ultrasound-mediated blood-brain barrier opening in vivo. J Cereb Blood Flow Metab. 2015;35:611–22.
23. Wang S, Olumolade OO, Sun T, et al. Noninvasive, neuron-specific gene therapy can be facilitated by focused ultrasound and recombinant adeno-associated virus. Gene Ther. 2015;22:104–10.
24. Thévenot E, Jordão JF, O'Reilly MA, et al. Targeted delivery of self-complementary adeno-associated virus serotype 9 to the brain, using magnetic resonance imaging-guided focused ultrasound. Hum Gene Ther. 2012;23:1144–55.
25. Nance E, Timbie K, Miller GW, et al. Non-invasive delivery of stealth, brain-penetrating nanoparticles across the blood-brain barrier using MRI-guided focused ultrasound. J Control Release. 2014;189:123–32.
26. Mead BP, Mastorakos P, Suk JS, et al. Targeted gene transfer to the brain via the delivery of brain-penetrating DNA nanoparticles with focused ultrasound. J Control Release. 2016;223:109–17.
27. Hersh DS, Nguyen BA, Dancy JG, et al. Pulsed ultrasound expands the extracellular and perivascular spaces of the brain. Brain Res. 2016;1646:543–50.
28. Wang S, Karakatsani ME, Fung C, et al. Direct brain infusion can be enhanced with focused ultrasound and microbubbles. J Cereb Blood Flow Metab. 2017;37:706–14.
29. Olbricht W, Sistla M, Ghandi G, et al. Time-reversal acoustics and ultrasound-assisted convection-enhanced drug delivery to the brain. J Acoust Soc Am. 2013;134:1569–75.
30. Mano Y, Saito R, Haga Y, et al. Intraparenchymal ultrasound application and improved distribution of infusate with convection-enhanced delivery in rodent and nonhuman primate brain. J Neurosurg. 2016;124:1490–500.
31. Liu Y, Paliwal S, Bankiewicz KS, et al. Ultrasound-enhanced drug transport and distribution in the brain. AAPS PharmSciTech. 2010;11:1005–17.

32. Lewis Jr. GK, Schulz ZR, Pannullo SC, et al. Ultrasound-assisted convection-enhanced delivery to the brain in vivo with a novel transducer cannula assembly. J Neurosurg. 2012;117:1128–40.
33. Chen H, Konofagou EE. The size of blood – brain barrier opening induced by focused ultrasound is dictated by the acoustic pressure. J Cereb Blood Flow Metab. 2014;34:1197–204.
34. Choi JJ, Member S, Feshitan JA, et al. Microbubble-Size Dependence of Focused Ultrasound-Induced Blood-Brain Barrier Opening in Mice In Vivo. IEEE Trans Biomed Eng. 2010;57:145–54.
35. Carpentier A, Canney M, Vignot A, et al. Clinical trial of blood-brain barrier disruption by pulsed ultrasound. Sci Transl Med. 2016;8:343re2.
36. Sheikov N, McDannold N, Vykhodtseva N, et al. Cellular mechanisms of the blood-brain barrier opening induced by ultrasound in presence of microbubbles. Ultrasound Med Biol. 2004;30:979–89.
37. Raymond SB, Treat LH, Dewey JD, et al. Ultrasound enhanced delivery of molecular imaging and therapeutic agents in Alzheimer's disease mouse models. PLoS One. 2008;3:e2175.
38. Jordão JF, Ayala-Grosso CA, Markham K, et al. Antibodies targeted to the brain with image-guided focused ultrasound reduces amyloid-β plaque load in the TgCRND8 mouse model of Alzheimer's disease. PLoS One. 2010;5:e10549.
39. Jordão JF, Thévenot E, Markham-Coultes K, et al. Amyloid-β plaque reduction, endogenous antibody delivery and glial activation by brain-targeted, transcranial focused ultrasound. Exp Neurol. 2013;248:16–29.
40. Nisbet RM, Van der Jeugd A, Leinenga G, et al. Combined effects of scanning ultrasound and a tau-specific single chain antibody in a tau transgenic mouse model. Brain. 2017:1–11.
41. Kobus T, Zervantonakis IK, Zhang Y, et al. Growth inhibition in a brain metastasis model by antibody delivery using focused ultrasound-mediated blood-brain barrier disruption. J Control Release. 2016;238:281–8.
42. Liu H-L, Hsu P-H, Lin C-Y, et al. Focused ultrasound enhances central nervous system delivery of Bevacizumab for malignant glioma treatment. Radiology. 2016;281:99–108.
43. Ziadloo A, Xie J, Frenkel V. Pulsed focused ultrasound exposures enhance locally administered gene therapy in a murine solid tumor model. J Acoust Soc Am. 2013;133:1827–34.
44. Chen P-Y, Hsieh H-Y, Huang C-Y, et al. Focused ultrasound-induced blood-brain barrier opening to enhance interleukin-12 delivery for brain tumor immunotherapy: a preclinical feasibility study. J Transl Med. 2015;13:93.
45. Alkins R, Burgess A, Ganguly M, et al. Focused ultrasound delivers targeted immune cells to metastatic brain tumors. Cancer Res. 2013;73:1892–9.
46. Alkins R, Burgess A, Kerbel R, et al. Early treatment of HER2-amplified brain tumors with targeted NK-92 cells and focused ultrasound improves survival. Neuro Oncol. 2016;18:974–81.
47. Kovacs ZI, Kim S, Jikaria N, et al. Disrupting the blood–brain barrier by focused ultrasound induces sterile inflammation. Proc Natl Acad Sci U S A. 2017;114:E75–84.
48. Liu H-L, Wai Y-Y, Hsu P-H, et al. In vivo assessment of macrophage CNS infiltration during disruption of the blood-brain barrier with focused ultrasound: a magnetic resonance imaging study. J Cereb Blood Flow Metab. 2010;30:177–86.
49. McMahon D, Bendayan R, Hynynen K. Acute effects of focused ultrasound-induced increases in blood-brain barrier permeability on rat microvascular transcriptome. Sci Rep. 2017;7:45657.
50. Dong Y, Benveniste EN. Immune function of astrocytes. Glia. 2001;36:180–90.
51. Ransohoff RM, Brown MA. Innate immunity in the central nervous system. J Clin Invest. 2012;122:1164–71.
52. Leinenga G, Götz J. Scanning ultrasound removes amyloid-β and restores memory in an Alzheimer's disease mouse model. Sci Transl Med. 2015;7:278ra33.
53. Hu Z, Yang XY, Liu Y, et al. Release of endogenous danger signals from HIFU-treated tumor cells and their stimulatory effects on APCs. Biochem Biophys Res Commun. 2005;335:124–31.
54. Kruse DE, Mackanos MA, O'Connell-Rodwell CE, et al. Short-duration-focused ultrasound stimulation of Hsp70 expression in vivo. Phys Med Biol. 2008;53:3641–60.
55. Madersbacher S, Gröbl M, Kramer G, et al. Regulation of heat shock protein 27 expression of prostatic cells in response to heat treatment. Prostate. 1998;37:174–81.
56. Wu F, Wang Z-B, Cao Y-D, et al. Expression of tumor antigens and heat-shock protein 70 in breast cancer cells after high-intensity focused ultrasound ablation. Ann Surg Oncol. 2007;14:1237–42.
57. Kramer G, Steiner GE, Gröbl M, et al. Response to sublethal heat treatment of prostatic tumor cells and of prostatic tumor infiltrating T-cells. Prostate. 2004;58:109–20.
58. Yuan S-M, Li H, Yang M, et al. High intensity focused ultrasound enhances anti-tumor immunity by inhibiting the negative regulatory effect of miR-134 on CD86 in a murine melanoma model. Oncotarget. 2015;6:37626–37.
59. Xia JZ, Xie FL, Ran LF, et al. High-intensity focused ultrasound tumor ablation activates autologous tumor-specific cytotoxic T lymphocytes. Ultrasound Med Biol. 2012;38:1363–71.
60. Deng J, Zhang Y, Feng J, et al. Dendritic cells loaded with ultrasound-ablated tumour induce in vivo specific antitumour immune responses. Ultrasound Med Biol. 2010;36:441–8.
61. Zhang Y, Deng J, Feng J, et al. Enhancement of antitumor vaccine in ablated hepatocellular carcinoma by high-intensity focused ultrasound. World J Gastroenterol. 2010;16:3584–91.
62. Yang R, Reilly CR, Rescorla FJ, et al. Effects of high-intensity focused ultrasound in the treatment of experimental neuroblastoma. J Pediatr Surg. 1992;27:246–51.
63. Yu H, Kortylewski M, Pardoll D. Crosstalk between cancer and immune cells: role of STAT3 in the tumour microenvironment. Nat Rev Immunol. 2007;7:41–51.
64. Huang X, Yuan F, Liang M, et al. M-HIFU inhibits tumor growth, suppresses STAT3 activity and enhances tumor specific immunity in a transplant tumor model of prostate cancer. PLoS One. 2012;7:e41632.
65. Liu F, Hu Z, Qiu L, et al. Boosting high-intensity focused ultrasound-induced anti-tumor immunity using a sparse-scan strategy that can more effectively promote dendritic cell maturation. J Transl Med. 2010;8:7.
66. Silvestrini MT, Ingham ES, Mahakian LM, et al. Priming is key to effective incorporation of image-guided thermal ablation into immunotherapy protocols. JCI Insight. 2017;2:e90521.
67. Hu Z, Yang XY, Liu Y, et al. Investigation of HIFU-induced anti-tumor immunity in a murine tumor model. J Transl Med. 2007;5:34.
68. Hunt SJ, Gade T, Soulen MC, et al. Antivascular ultrasound therapy: magnetic resonance imaging validation and activation of the immune response in murine melanoma. J Ultrasound Med. 2015;34:275–87.
69. Bandyopadhyay S, Quinn TJ, Scandiuzzi L, et al. Low-intensity focused ultrasound induces reversal of tumor-induced T cell tolerance and prevents immune escape. J Immunol. 2016;196:1964–76.
70. Kheirolomoom A, Ingham ES, Mahakian LM, et al. CpG expedites regression of local and systemic tumors when combined with activatable nanodelivery. J Control Release. 2015;220:253–64.
71. Lu P, Zhu XQ, Xu ZL, et al. Increased infiltration of activated tumor-infiltrating lymphocytes after high intensity focused ultrasound ablation of human breast cancer. Surgery. 2009;145:286–93.
72. Wu F, Wang ZB, Lu P, et al. Activated anti-tumor immunity in cancer patients after high intensity focused ultrasound ablation. Ultrasound Med Biol. 2004;30:1217–1222.
73. Xu Z-L, Zhu X-Q, Lu P, et al. Activation of tumor-infiltrating antigen presenting cells by high intensity focused ultrasound ablation of human breast cancer. Ultrasound Med Biol. 2009;35:50–7.
74. Zhou Q, Zhu X-Q, Zhang J, et al. Changes in circulating immunosuppressive cytokine levels of cancer patients after high intensity focused ultrasound treatment. Ultrasound Med Biol. 2008;34:81–7.
75. Wyss-Coray T, Rogers J. Inflammation in Alzheimer disease-a brief review of the basic science and clinical literature. Cold Spring Harb Perspect Med. 2012;2:a006346.
76. Jackson CM, Kochel CM, Nirschl CJ, et al. Systemic tolerance mediated by melanoma brain tumors is reversible by radiotherapy and vaccination. Clin Cancer Res. 2016;22:1161–72.
77. Pardoll DM. The blockade of immune checkpoints in cancer immunotherapy. Nat Rev Cancer. 2012;12:252–64.
78. Reardon DA, Gokhale PC, Klein SR, et al. Glioblastoma eradication following immune checkpoint blockade in an orthotopic, immunocompetent model. Cancer Immunol Res. 2016;4:124–35.
79. Kjærgaard J, Tanaka J, Kim JA, et al. Therapeutic efficacy of OX-40 receptor antibody depends on tumor immunogenicity and anatomic site of tumor growth. Cancer Res. 2000;60:5514–21.
80. Margolin K, Ernstoff MS, Hamid O, et al. Ipilimumab in patients with melanoma and brain metastases: An open-label, phase 2 trial. Lancet Oncol. 2012;13:459–65.
81. Wainwright DA, Chang AL, Dey M, et al. Durable therapeutic efficacy utilizing combinatorial blockade against IDO, CTLA-4, and PD-L1 in mice with brain tumors. Clin Cancer Res. 2014;20:5290–301.
82. Fecci PE, Ochiai H, Mitchell DA, et al. Systemic CTLA-4 blockade ameliorates glioma-induced changes to the CD4 + T cell compartment without affecting regulatory T-cell function. Clin Cancer Res. 2007;13:2158–67.
83. Treat LH, McDannold N, Zhang Y, et al. Improved anti-tumor effect of liposomal doxorubicin after targeted blood-brain barrier disruption by MRI-guided focused ultrasound in rat glioma. Ultrasound Med Biol. 2012;38:1716–25.
84. Aryal M, Vykhodtseva N, Zhang YZ, et al. Multiple treatments with liposomal doxorubicin and ultrasound-induced disruption of blood-tumor and blood-brain barriers improve outcomes in a rat glioma model. J Control Release. 2013;169:103–11.
85. Aryal M, Vykhodtseva N, Zhang Y-Z, et al. Multiple sessions of liposomal doxorubicin delivery via focused ultrasound mediated blood-brain barrier disruption: a safety study. J Control Release. 2015;204:60–9.
86. Aryal M, Park J, Vykhodtseva N, et al. Enhancement in blood-tumor barrier permeability and delivery of liposomal doxorubicin using focused ultrasound and microbubbles: evaluation during tumor progression in a rat glioma model. Phys Med Biol. 2015;60:2511–27.
87. Bernstein MB, Garnett CT, Zhang H, et al. Radiation-induced modulation of costimulatory and coinhibitory T-cell signaling molecules on human prostate carcinoma cells promotes productive antitumor immune interactions. Cancer Biother Radiopharm. 2014;29:153–61.
88. Gameiro SR, Malamas AS, Bernstein MB, et al. Tumor cells surviving exposure to proton or photon radiation share a common immunogenic modulation

signature, rendering them , more sensitive to T cell-mediated killing. Int J Radiat Oncol Biol Phys. 2016;95:120–30.
89. Gameiro SR, Higgins JP, Dreher MR, et al. Combination therapy with local radiofrequency ablation and systemic vaccine enhances antitumor immunity and mediates local and distal tumor regression. PLoS One. 2013;8:e70417.
90. Chakravarty PK, Guha C, Alfieri A, et al. Flt3L therapy following localized tumor irradiation generates long-term protective immune response in metastatic lung cancer: Its implication in designing a vaccination strategy. Oncology. 2006;70:245–54.
91. Hannan R, Zhang H, Wallecha A, et al. Combined immunotherapy with Listeria monocytogenes-based PSA vaccine and radiation therapy leads to a therapeutic response in a murine model of prostate cancer. Cancer Immunol Immunother. 2012;61:2227–38.
92. Chakravarty PK, Alfieri A, Thomas EK, et al. Flt3-ligand administration after radiation therapy prolongs survival in a murine model of metastatic lung cancer. Cancer Res. 1999;59:6028–32.
93. Belcaid Z, Phallen JA, Zeng J, et al. Focal radiation therapy combined with 4-1BB activation and CTLA-4 blockade yields long-term survival and a protective antigen-specific memory response in a murine glioma model. PLoS One. 2014;9:e101764.
94. Zeng J, See AP, Phallen J, et al. Anti-PD-1 blockade and stereotactic radiation produce long-term survival in mice with intracranial gliomas. Int J Radiat Oncol Biol Phys. 2013;86:343–9.
95. Kim JE, Patel MA, Mangraviti A, et al. Combination therapy with anti-PD-1, anti-TIM-3, and focal radiation results in regression of murine gliomas. Clin Cancer Res. 2017;23:124–36.
96. Patel MA, Kim JE, Theodros D, et al. Agonist anti-GITR monoclonal antibody and stereotactic radiation induce immune-mediated survival advantage in murine intracranial glioma. J Immunother Cancer. 2016;4:28.
97. Hodge JW, Guha C, Neefjes J, et al. Synergizing radiation therapy and immunotherapy for curing incurable cancers: opportunities and challenges. Oncology (Williston Park). 2008;22:1064–84.
98. Derer A, Frey B, Fietkau R, et al. Immune-modulating properties of ionizing radiation: rationale for the treatment of cancer by combination radiotherapy and immune checkpoint inhibitors. Cancer Immunol Immunother. 2016;65:779–86.
99. D'Souza NM, Fang P, Logan J, et al. Combining radiation therapy with immune checkpoint blockade for central nervous system malignancies. Front Oncol. 2016;6:212.